Smoothing out HLLC's "carbuncles" in Fluid Shock Simulations

Xander Jenkin

August 2, 2022

Abstract

Many fluid shock simulations use approximate Riemann solvers to compute the flux of the fluid at a given resolution. One common approximate Riemann solver is HLL (Harten, Lax and van Leer), which computes the flux in a cell by comparing the left and right sound speeds of the fluid. HLLC (HLL + Contact) is a modificiation of HLL that adds an additional point of contact—the transverse sound speed S_M—in-between the left and right. This extra point of contact allows for higher fidelity and more details at the same resolution as HLL, making it a good, inexpensive modification to make an approximate Riemann solver more accurate. However, HLLC has an instability, the "carbuncle" instability, which adds additional erroneous noise to the simulation, growing exponentially over time and distorting the shape of the fluid. In this paper, we quantify the error produced by these carbuncles and introduce an error correction factor of θ to help negate the effect of the carbuncles, creating the new modified LHLLC Riemann solver. This new Riemann solver is able to resolve finer details due to the lower diffusivity of the extra contact term S_M without the carbuncles present in HLLC.

1 Introduction

When rendering fluid shock simulations, the main issue to solve is the Riemann problem: computed using (in this case, approximate) Riemann solvers. One Riemann solver is HLL (Harten, Lax and van Leer), which takes the left and right sound speeds S_L and S_R uses them to compute the flux in a given cell. The flux can then be used to derive the mass, momentum, and energy of the fluid in a given cell, which the simulation uses to draw how the fluid is moving once all the cells' fluxes are calculated. A modification to this scheme adds an additional point of contact, S_M, the transverse velocity between S_L and S_R, making the approximate solver more accurate to an exact Riemann solver (while requiring much less computational power), and revealing more details not present in HLL. This modification to HLL is called HLLC, adding a "C" for the additional point of contact provided in S_M. This should mean that HLLC would be able to reveal more details in complex fluid simulations than what HLL is capable of, but there is an instability unique to HLLC: The "carbuncle" instability, which adds additional noise to the simulation and makes details that would otherwise be accurate erroneous and unclear. This paper seeks to identify, quantify, and fix the carbuncles so that more fluid simulations can be run with higher fidelity and finer details that were not previously present.

2 Perturbing Initial Conditions to Stimulate Carbuncles

The "carbuncle" instability erroneously increases the velocity of cells, so we can quantify it by tracking the maximum velocity in the y-direction of a 1-D shock moving in the x-direction (naturally, this should not have any y-velocity at all). If we run this simulation with zero y-velocity, though, HLLC does not produce any carbuncle instabilities in the y-direction, so we need to perturb the y-velocity by a small amount to give it some value, after which the instability should form. We can do this by giving each cell of the shock an initial y-velocity set to a random value from $0.5 \times 10^{-}3$ to $-0.5 \times 10^{-}3$ [1]. When we measure the maximum y-velocity of the cells as a function of time, it should be relatively stable at a low value without the instability. As the instability grows, so too should the y-velocity.

3 1-D Planar Shock Test

We have set up a leftward-moving shockwave that has a density of $\frac{160}{27} \approx 5.926$ with an x-velocity of $\frac{133\sqrt{1.4}}{8} \times c_s \approx 19.671 \times c_s$ (where the sound speed $c_s = 1$) into a lower-density zone of 1.0. This simulation has 100 timesteps from $t = 1$ to $t = 100$.

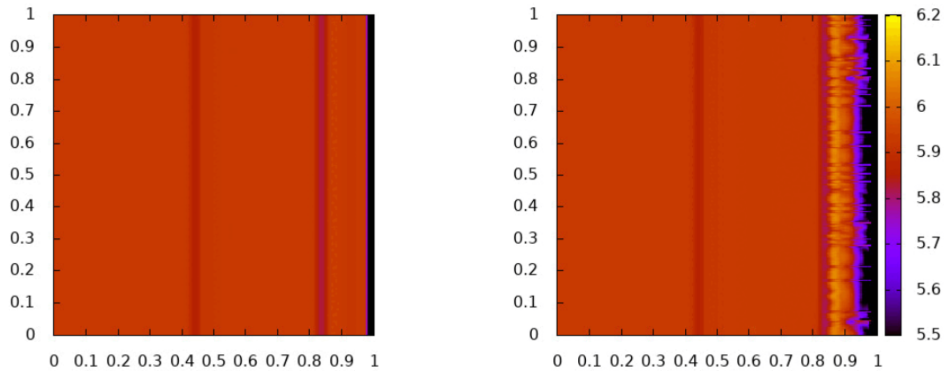

Figure 1: HLL and HLLC in the 1-D planar shock test, $t = 90$

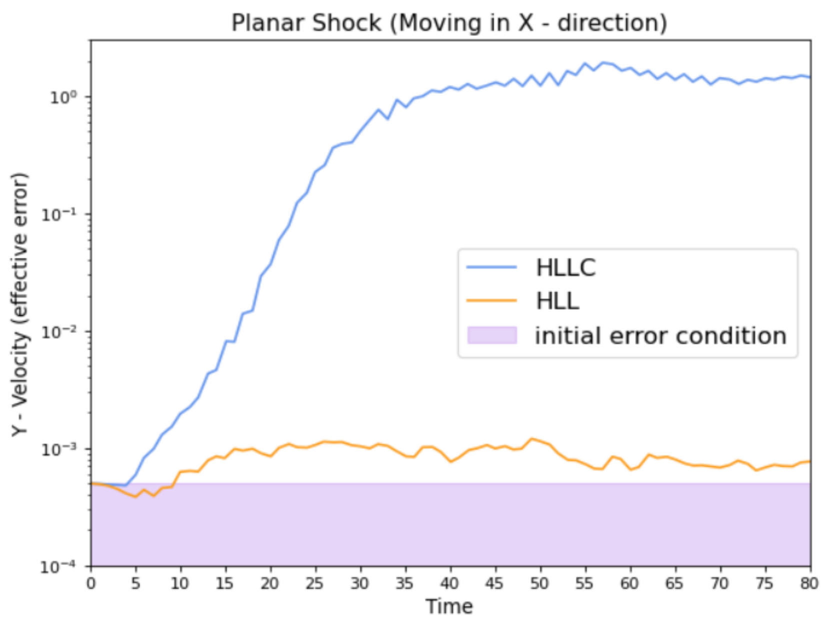

Figure 2: Maximum normal y-velocity over time

In the plot of the maximum y-velocity over time, we can see that HLLC has an error that grows exponentially before petering off at around $t = 35$, while HLL has little to no overall trend over time, with y-velocity consistently below 10^{-3} (which is very close to the initial perturbation, where it should be without the carbuncles).

4 Density Step Test

From the previous test, it is clear that HLL gives a much more accurate render than HLLC, but that was in a uniform density field. This next test showcases a non-uniform density field, with the density being $\rho = 1.0$ to the left of the middle and $\rho = 0.5$ to the right of the middle.

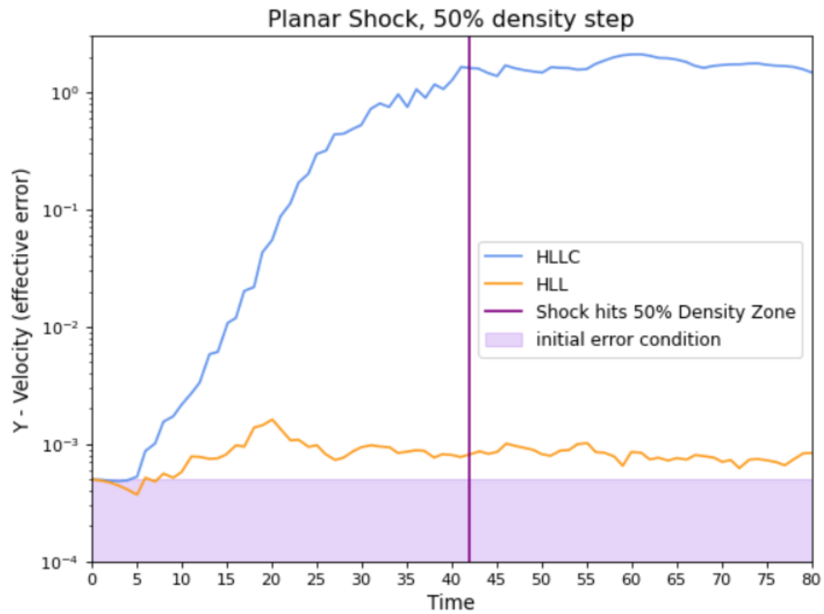

Figure 3: Maximum normal y-velocity over time

This test did not reveal anything new (with the snapshots omitted for brevity), and the y-velocity plot (shown above) also does not reveal the low-diffusivity benefits of HLLC over HLL. The main benefit of HLLC is in the finer details in the shapes created by non-uniform shock collisions, so we can see these details by making the density step non-uniform.

5 Sinusoid Step Test

In this next simulation, we changed the density step to a sinusoidal step, where we can see some of the differences in shape between HLL and HLLC, and how they react to a non-uniform density step.

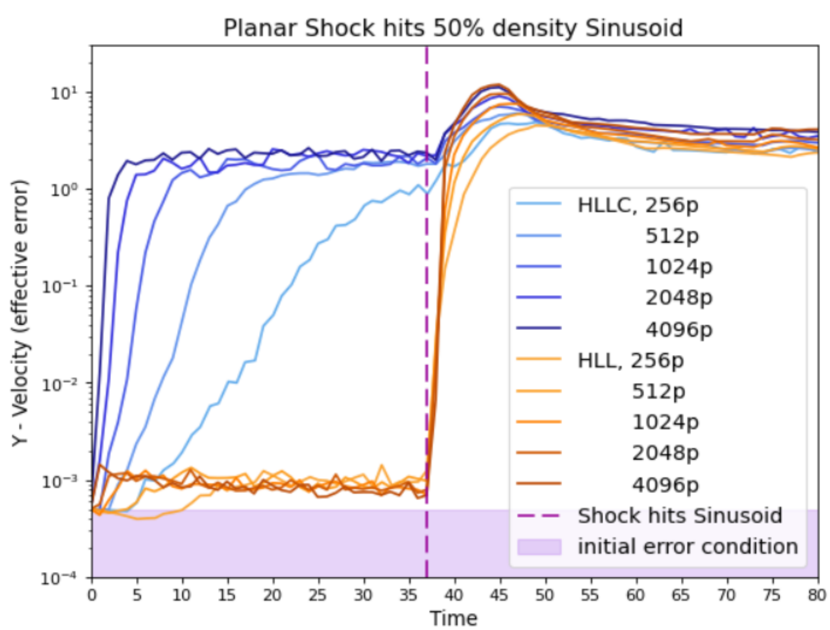

Figure 4: Maximum normal y-velocity over time

Here, we can see how the carbuncles scale with resolution, as the exponential growth in HLLC becomes sharper as we increase the resolution—HLL does not scale with resolution, and only increases in y-velocity upon hitting the sinusoid, after which the y-velocity is no longer an effective measurement of error.

Before we view the images, we moved the sinusoid over from the middle to the left, so we can see the shapes produced develop for longer, and reveal some of the finer details.

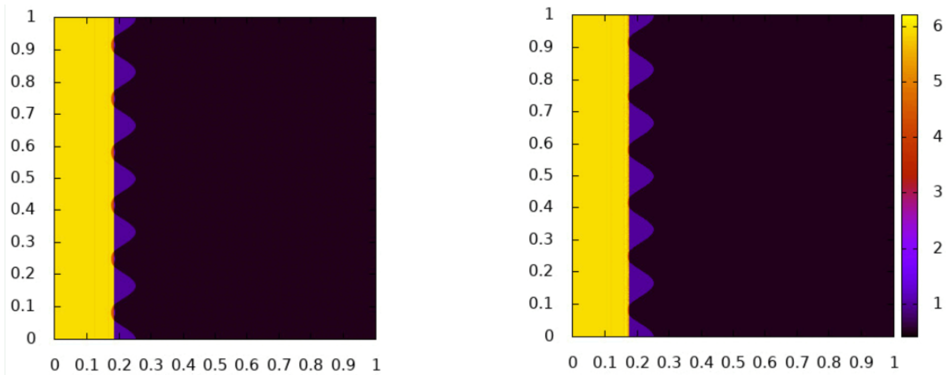

Figure 5: HLL and HLLC in the Sinusoid step test, $t = 10$

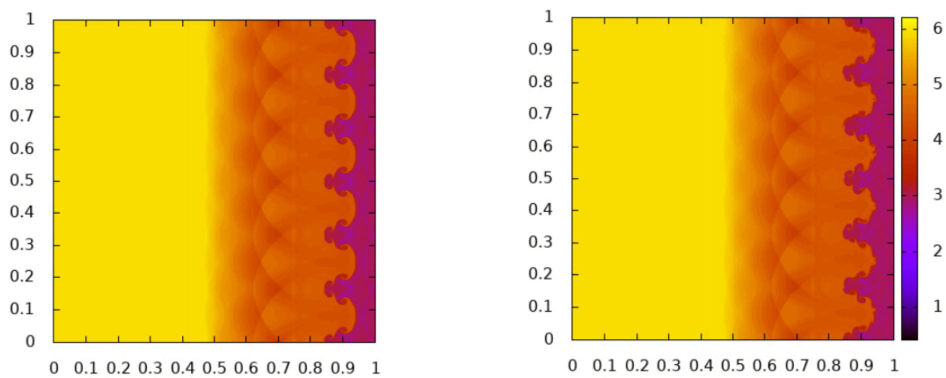

Figure 6: HLL and HLLC in the Sinusoid step test, $t = 90$

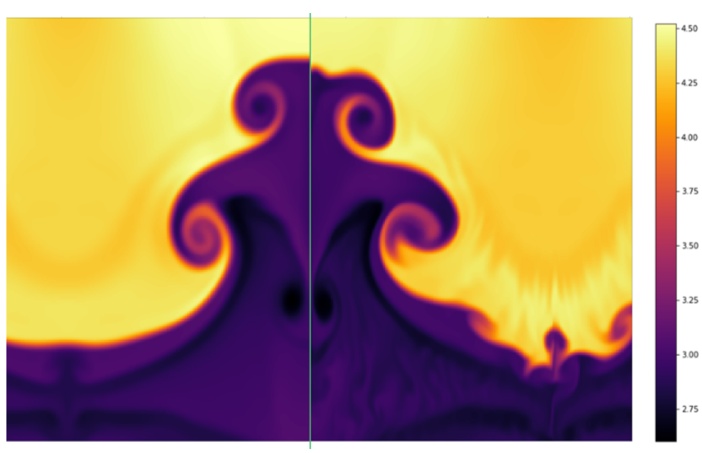

Figure 7: HLL and HLLC in the Sinusoid step test, $t = 90$

Taking a closer look at the mushroom clouds (in a split view, shown above), we can see that HLLC provides more detail than HLL, but at the cost of a mangled shape due to the carbuncles. Higher fidelity due to the extra S_M term is a benefit of HLLC, but we must correct for the carbuncles if we want to see these details without the effects of the carbuncles.

6 Quantifying the Carbuncles

In order to create a fix to HLLC to correct for the carbuncles, we need to quantify exactly how they grow, in relation to the given parameters of our test and how it scales to the resolution at which the test is being rendered.

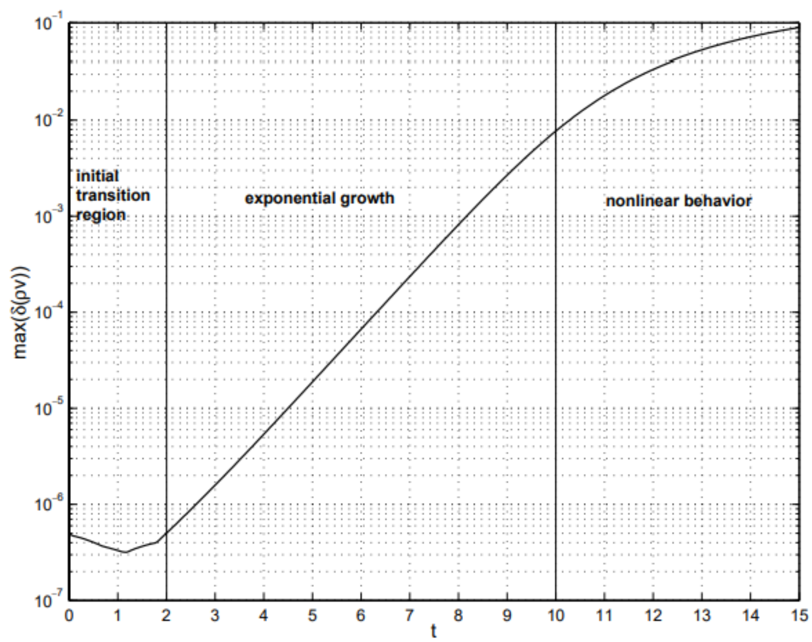

Figure 8: Exponential growth of the instability [2]

Above is a theorized model of how the carbuncle instability grows over time, with the middle portion being an exponential of the form $\|\mathbf{V_y}\| = V_0 exp(A\frac{c_s}{\Delta x}(t - t_0))$

We can plug in values for many of the given variables, which are related to the quantities and initial conditions of our simulation.

$V_0 = \text{initial error} = 0.5 \times 10^{-3}$, $\Delta x = \frac{boxlen}{resolution} = \frac{2400}{resolution} = \frac{2400}{2^{level}}$, $t_0 = \frac{2^{10}}{level} = \frac{1024}{level}$, $c_s = 1$

Finding that, for our simulations,

$\|\mathbf{V_y}\| = 0.5 \times 10^{-3} exp(A\frac{resolution}{2400}(t - \frac{1024}{level}))$

Where the only two free parameters are the resolution/level and a growth rate A.

We can plot this function for the middle exponential section for all levels to find a best fit estimate for the value of A_0, which is shown below, with $\|\mathbf{V_y}\|$ over-plotted for resolution levels 8-12, with the region between $A_{\min}$ and $A_{\max}$ filled in. We find that the growth rate of the carbuncles A is somewhere between 2 and 3, which is useful because this quantity is consistent regardless of the resolution (which is not true about the carbuncles, and should be true about our fix to eliminate the carbuncles).

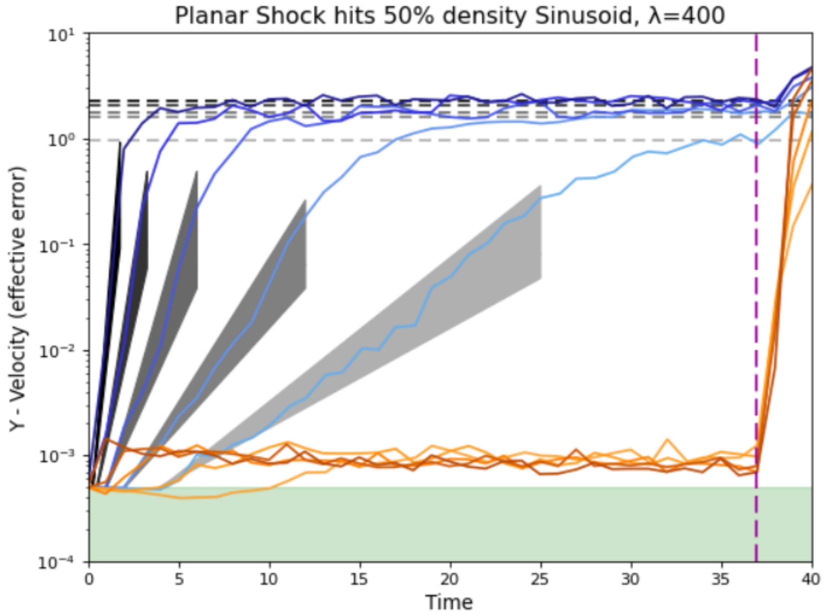

Figure 9: $A_{min} \approx 2.0408, A_{max} \approx 2.9411$

7 Modifying the Riemann Solver

A way to remedy the carbuncle instability is to introduce an error correction factor that raises/lowers the middle calculation for the fluid velocity to compensate for the errors. We calculate this factor θ by taking into account the velocities of both the immediate and adjacent cells around the current cell. Continuously applying this to all cells should stop carbuncle instabilities from developing.

$$
\begin{aligned}
S_M &= \frac{(S_R - u_R)\rho_R u_R - (S_L - u_L)\rho_L u_L - \theta(P_{tR} - P_{tL})}{(S_R - u_R)\rho_R - (S_L - u_L)\rho_L}, \\
\theta &= \min\left(1, \frac{-\min(\Delta u, 0) + c_{f,\max}}{-\min(\Delta v, \Delta w, 0) + c_{f,\max}}\right)^a, \\
\Delta u &= u_{i+1,j,k} - u_{i,j,k}, \\
\Delta v &= \min(v_{i,j,k} - v_{i,j-1,k}, v_{i,j+1,k} - v_{i,j,k}, \\
&\quad v_{i+1,j,k} - v_{i+1,j-1,k}, v_{i+1,j+1,k} - v_{i+1,j,k}), \\
\Delta w &= \min(w_{i,j,k} - w_{i,j,k-1}, w_{i,j,k+1} - w_{i,j,k}, \\
&\quad w_{i+1,j,k} - w_{i+1,j,k-1}, w_{i+1,j,k+1} - w_{i+1,j,k}),
\end{aligned}
$$

Figure 10: HLLD scheme's implementation of θ [3]. For our testing, we used $a = 4$.

Modifying the HLLC scheme with this fix, we re-ran all of the previous tests with this new Riemann solver (LHLLC), with the goal of keeping the low-diffusivity of HLLC with the low instability of HLL.

8 Results

8.1 Planar Shock Test

We re-ran the first planar shockwave test in uniform density with LHLLC, and the carbuncles appear to be eliminated (figure below at $t = 90$).

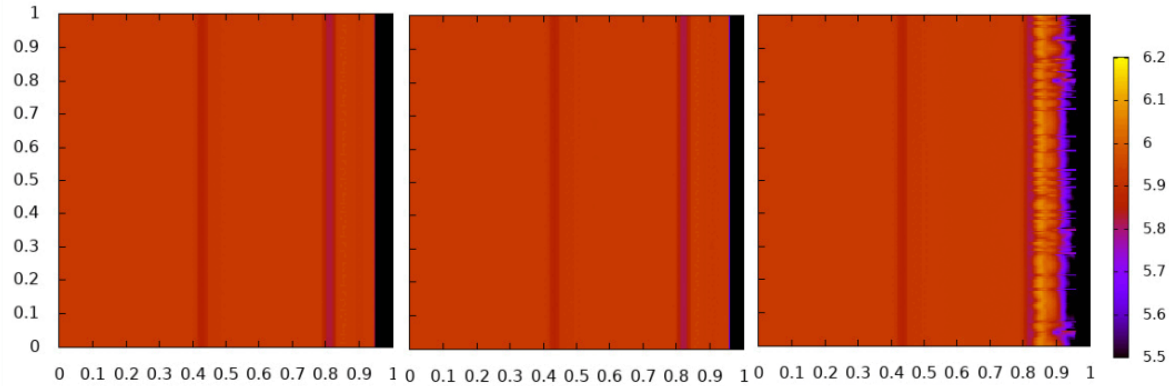

Figure 11: (from left to right) HLL, LHLLC, and HLLC in the planar shock test in uniform density

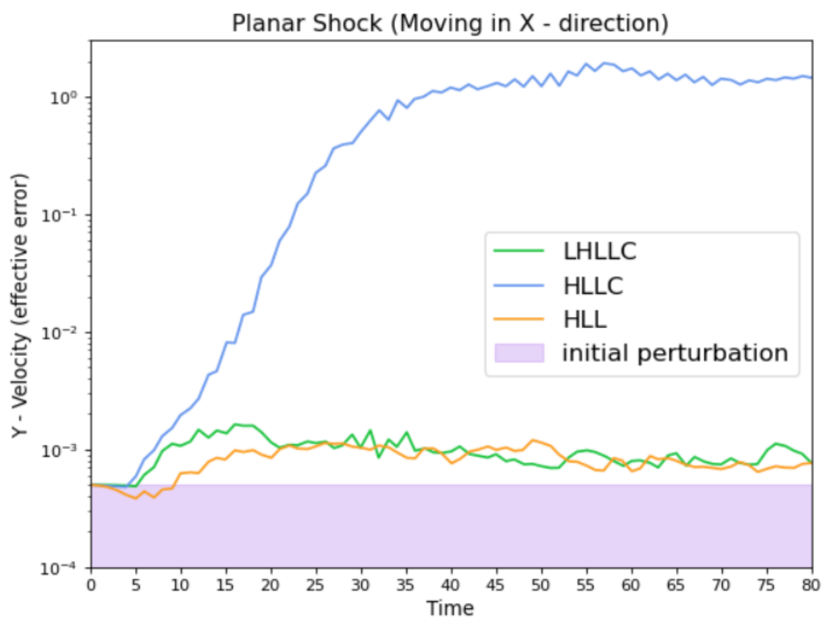

Figure 12: Maximum normal y-velocity over time

When measuring the y-velocity over time, LHLLC performs as well as HLLC, with no increasing trend in y-velocity over time.

8.2 Sinusoid Test

In the Sinusoid test, LHLLC once again shows no increase in y-velocity over time, and the rate of increase of its y-velocity upon hitting the sinusoid does not correlate with higher resolutions, similar to HLL.

When qualitatively viewing the diffusivity of the solvers in the sinusoid test, LHLLC holds up well (pictured below).

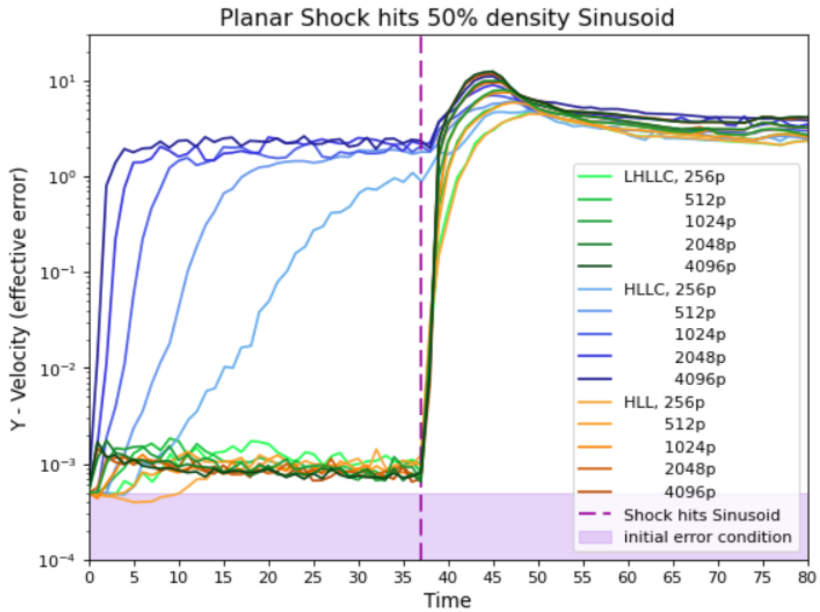

Figure 13: Maximum normal y-velocity over time

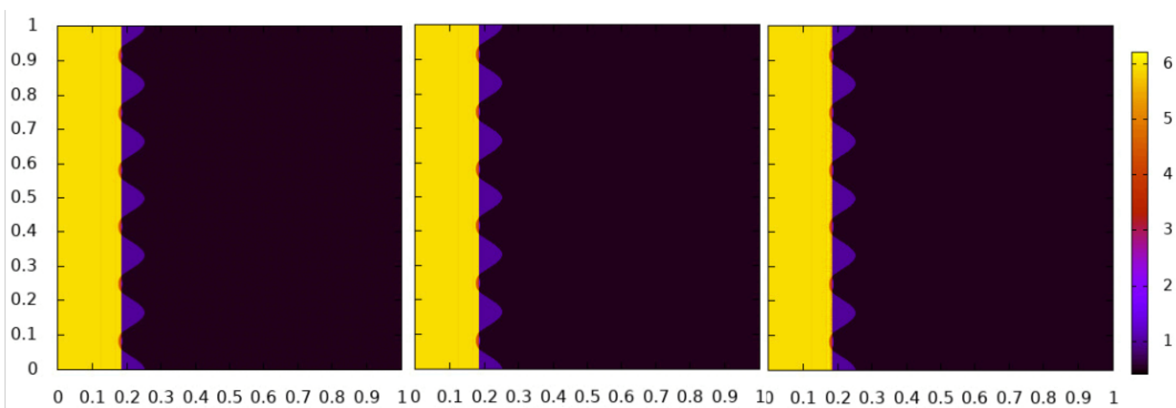

Figure 14: HLL, LHLLC, and HLLC in the sinusoid density step test, $t = 10$

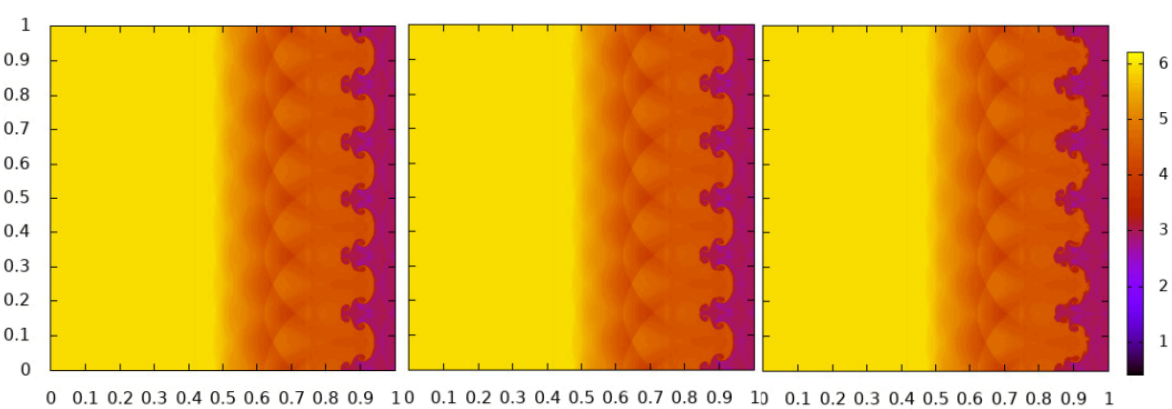

Figure 15: HLL, LHLLC, and HLLC in the sinusoid density step test, $t = 90$

Zooming into the mushroom clouds, LHLLC provides a nice sharpness not present in HLL due to the low diffusivity of the additional S_M contact term, without any of the nasty distortion effects due to the carbuncles present in HLLC.

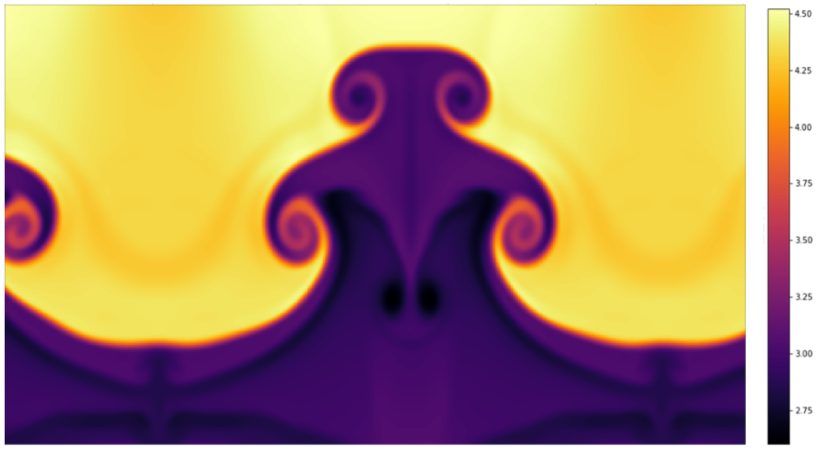

Figure 16: Close-up of HLL in the sinusoid density step test, $t = 90$

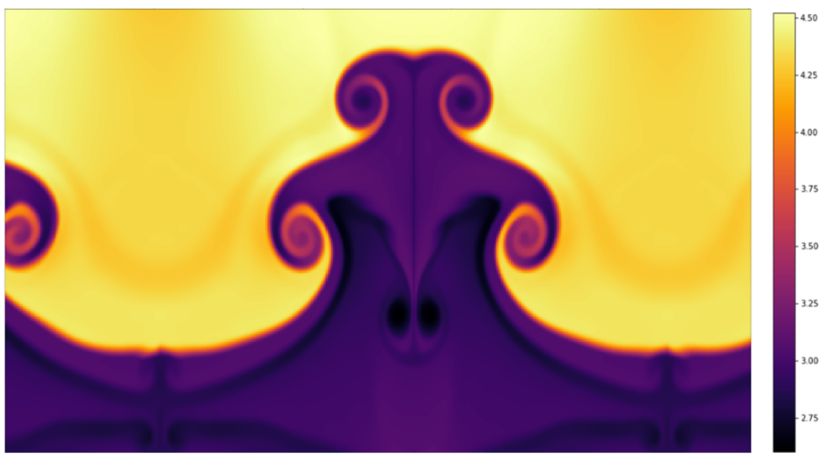

Figure 17: Close-up of LHLLC in the sinusoid density step test, $t = 90$

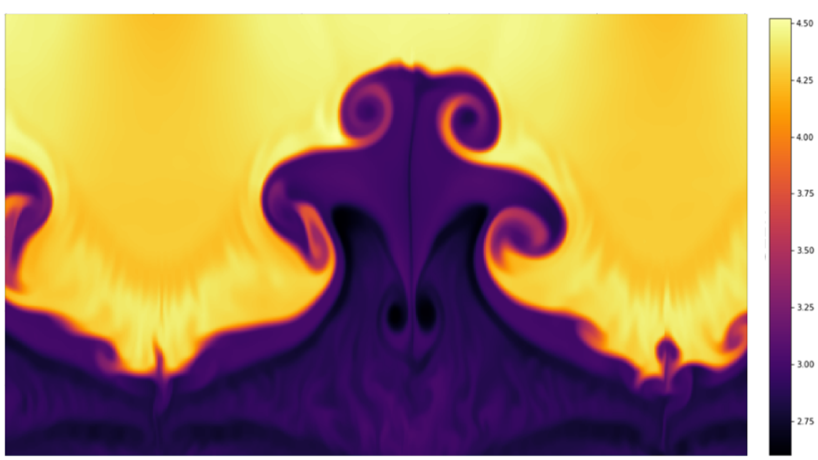

Figure 18: Close-up of HLLC in the sinusoid density step test, $t = 90$

8.3 Future implications

The extra diffusivity of S_M and removal of the carbuncle instability due to the θ factor means that LHLLC can be used to run higher fidelity fluid shock simulations in RAMSES, both planar and radial. In the future, we will conduct more simulations to continue to test the consistency of LHLLC and seek to reveal new details in high-resolution fluid simulations (the ones most plagued by the carbuncles) that were previously not apparent.

References

[1] Nico Fleischmann, Stefan Adami, and Nikolaus A. Adams. A shock-stable modification of the HLLC Riemann solver with reduced numerical dissipation. *Journal of Computational Physics*, 423:109762, December 2020.

[2] Michael Dumbser, Jean-Marc Moschetta, and Jérémie Gressier. A matrix stability analysis of the carbuncle phenomenon. *Journal of Computational Physics*, 197(2):647–670, July 2004.

[3] Takashi Minoshima and Takahiro Miyoshi. A low-dissipation HLLD approximate Riemann solver for a very wide range of Mach numbers. *Journal of Computational Physics*, 446:110639, December 2021.